ELSEVIER

International Journal of Mass Spectrometry 190/191 (1999) 153–160

International Journal of Mass Spectrometry

Cooling of mass-separated beams using a radiofrequency quadrupole ion guide

M.D. Lunney*[,a], R.B. Moore[b]

[a]*Centre de Spectrométrie Nucléaire et de Spectrométrie de Masse, Université Paris Sud, F-91405 Orsay, France*
[b]*Department of Physics, McGill University, 3600 University Street, Montreal H3A 2B1, Canada*

Received 5 November 1998; accepted 31 December 1998

Abstract

A simulation is presented of a radiofrequency quadrupole rod system operated in the presence of He buffer gas for cooling a mass separated, decelerated ionic beam and thus, reducing its emittance. This system is being developed to benefit the sensitivity of on-line experiments using weak beams of radioactive isotopes. The numerical integration algorithm incorporates a viscous damping force modeled by a fit of mobility data of ions in a light neutral gas. Results indicate that an emittance reduction of almost 2 orders of magnitude in all coordinates is possible with near 100% transmission barring charge exchange and molecular formation. (Int J Mass Spectrom 190/191 (1999) 153–160) © 1999 Elsevier Science B.V.

Keywords: Radiofrequency quadrupole mass filter; Buffer-gas cooling; Beam optics; Ion mobility; Mass spectrometry

1. Introduction

For most experiments using weak radioactive beams it is desirable that the beam emittance be as small as possible. The MISTRAL experiment at the CERN isotope mass separator facility ISOLDE [1] is particularly affected since it is a transmission spectrometer. A small emittance means that the beam is concentrated in a small geometrical area, with a small angular divergence, and a small energy spread. A small emittance generally permits a more precise measurement and the way to reduce it is to cool the beam. Several cooling schemes exist: stochastic cooling and electron cooling are generally used in storage rings while ion trapping applications rely on resistive cooling, laser cooling, and buffer-gas cooling. The latter is of great interest as it is relatively simple and more or less universal. The only major drawback of buffer gas is that ions can undergo charge exchange or molecular formation, in which case they are lost. A short review can be found in [2].

Ions confined in a Paul or Penning trap can be cooled by introducing a light, neutral gas such as H_2 or He. The ion motion is viscously damped, in principle down to the temperature of the gas itself. This scheme was extended to a continuous beam traversing a radiofrequency quadrupole (RFQ) by Douglas and French [3] who demonstrated a dramatic gain in transmission through a small hole at the end of a gas-filled quadrupole followed by a mass-resolving quadrupole. The quadrupole provides a time-average confining force in order to avoid the diffusion that would otherwise occur as the ions transit the gas.

* Corresponding author. E-mail: lunney@csnsm.in2p3.fr

Dedicated to J.F.J. Todd and R.E. March in recognition of their original contributions to quadrupole ion trap mass spectrometry.

PII S1387-3806(98)00009-3

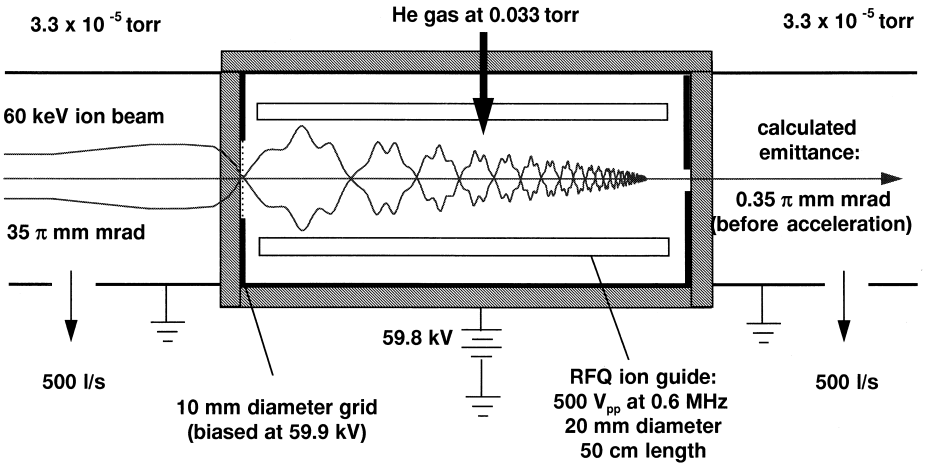

Fig. 1. Schematic diagram of the ion guide beam cooling system. The details of the deceleration system are not shown nor are those of the mass filter housing nor extraction electrodes. Detailed description and selection criteria for all numbers are given in the text.

Similar work using sextupole ion guides has previously been reported [4,5].

The purpose of the simulation presented here is to design a similar system capable of decelerating the 60 keV ISOLDE beam and cooling it to the buffer gas temperature before reacceleration. Since radionuclides are generally short-lived, the cooling processes must be rapid. Furthermore, the losses incurred by such a maneuver must be minimal. In principle, simply increasing the buffer gas pressure will increase the cooling rate. However the consequences of operating electric devices at high pressure are obvious. Such a design requires detailed simulation of a system of quadrupole rods (which we refer to as an rf ion guide) and the cooling mechanism. The simulation of the overall process was done in two steps. An electrostatic deceleration system was designed using the SIMION program and the transverse emittance at the entrance to the mass filter was extracted. The evolution of this phase space diagram in the ion guide is then computed using a fifth-order Runge–Kutta integration. A damping term, subtracted from the acceleration term of the direct equations of motion, is calculated (for a specified temperature and pressure) using a fit of measured mobility data for a given ionic species in a given gas. Note that it is the ion mobility that enables more accurate simulation of viscous damping as opposed to spherical "hard-ball" collisions (as explained later). In addition, a residual energy term is added to the acceleration term corresponding to the buffer gas temperature (preventing the unrealistic situation in which the ions are cooled to zero temperature). Finally, the resulting (reduced) phase space diagram can be directly compared with that of the input beam.

2. Schematic layout of apparatus

Shown in Fig. 1 is a schematic diagram of the beam cooling system. As this system is designed for the 60 keV ISOLDE beam, the measured emittance [6] of 35 π mm mrad was used for the simulation. Given pumping speeds of 500 L/s, the end pressures are calculated from Knudsen's formula [Eq. (1)] assuming a set of enclosed rods 50 cm long with a 10 mm diaphragm with 0.033 Torr of gas introduced in the center. The ion trajectories are those simulated by the program (using the mass filter operating parameters indicated) and show that the ions reach thermal equilibrium with the gas while inside the mass filter. The ions' initial conditions are determined by the initial beam spot size and consequent divergence (from Liouville's theorem) as calculated by SIMION. Furthermore, the effect of the rf phase on the ion injection (due to rf distortion) has been minimized by

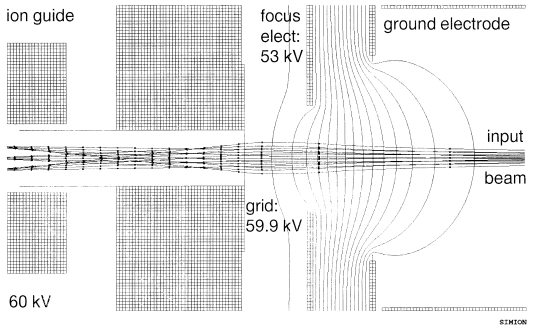

Fig. 2. Electrode configuration for decelerating the 60 kV ISOLDE beam and injecting it into the rf ion guide system at about 130 eV. The first electrode (right) is at ground potential and has an aperture of 40 mm. The focus electrode, located 40 mm downstream with a 30 mm aperture, is at 53 kV. A further axial gap of 40 mm separates the injection aperture grid of 10 mm diameter which floats at 59.9 kV. The grid is necessary to prevent overfocusing. The ion guide is located 80 mm further and floats at 60 kV. The beam focus, given the initial emittance of 35 π mm mrad at 60 kV, is about 7 mm in diameter with a divergence of about 15° (corresponding to a transverse energy of about 8.5 eV).

choosing a large rf frequency and keeping the rf voltage as low as possible (here we are limited by the radial well depth which must be deep enough to contain the ions that are radialy defocused after deceleration and injection) to maximize transmission.

3. Detailed description of the simulation

3.1. Deceleration system

The deceleration system was modeled using the SIMION program, a graphical interface that uses a finite difference solution technique for solving electrostatic boundary value problems and a Runge–Kutta numerical integration for the ion trajectories. The goal of this system is to decelerate a 60 keV ion beam to about 100–200 eV maintaining a moderate focus into the mass filter aperture. This can be achieved using a gradual intermediate deceleration as shown in Fig. 2. The transverse phase space diagram at the entrance to the rf ion guide is then extracted for subsequent computation.

3.2. RFQ mass filter (ion guide)

A detailed introduction to the RFQ mass filter is given by Dawson [7]. It consists of two pairs of equidistant and parallel rods. A rf voltage is applied to opposing rod pairs such that each is 180° out of phase. This creates a quadrupole field (which is zero along the central axis) that alternately focuses in each transverse direction with no axial field component. The operating parameters of the mass filter are governed by the so-called Mathieu parameters a and q which are defined as:

$$a = \frac{8eU}{mx_0^2\Omega^2} \qquad q = \frac{4eV}{mx_0^2\Omega^2} \tag{1}$$

for an ion of charge e, mass m in a mass filter of rod separation $2x_0$ operated with the applied potential $U - V \cos \Omega t$, where V is the zero-to-peak voltage applied at frequency Ω. The static potential U is used to increase the filtering effect (mass resolution) but this comes at the expense of transmission. In our case, $U = 0$ for maximum transmission and hence, we refer to the mass filter rather as an ion guide. When the driving force is modest (i.e. for values of $q < 0.4$) the resultant ion motion is essentially that of a simple harmonic oscillator (macromotion) slightly modulated by the driving rf frequency (micromotion).

In order to study ion beam dynamics it is important to introduce the notion of phase space: the two-dimensional space comprised of the canonically conjugate coordinates momentum and displacement (units of *action*). A good way to imagine such a representation for an ion in a quadrupole is to use the phase space diagram of a simple harmonic oscillator as shown in Fig. 3. The trajectory in phase space follows one elliptical path going clockwise. The maximum displacement corresponds to the point where the velocity is zero, whereas the zero displacement axis is crossed with maximum velocity. To represent a group of ions in the ion guide, a phase space diagram is used together with a thermodynamic (Gibbs) distribution, also shown in Fig. 3 expressed in Gaussian form. For more details see references [8,9]. Such an ellipse is generated by the SIMION program (itself given an input ellipse) and used as a starting

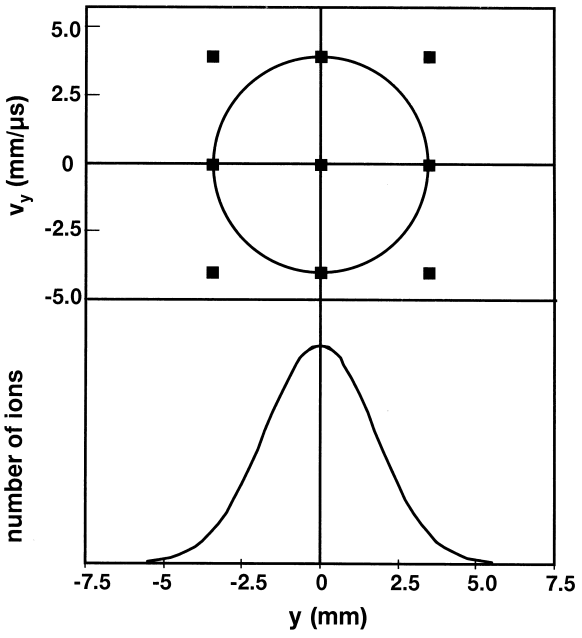

Fig. 3. Phase space (action) diagram for a simple harmonic oscillator. Strictly speaking, the vertical axis should be momentum but is here plotted versus velocity (divergence is also sometimes used). The nine points represent the discretization of the phase space ellipse envelope. Shown below is a Gaussian (Gibbs) distribution used to describe the ion density inside the action diagram.

point for the numerical integration through the ion guide.

3.3. rf distortion and the ion guide injection aperture

Due to the phenomenon of rf distortion, the acceptance of a rf ion guide is limited and furthermore, depends on the phase of the rf voltage at injection. This means that the transmission is not uniform with time. The ion motion is not exactly simple harmonic but modulated by the rf which has the effect of squeezing and twisting the elliptical phase space diagram shown in Fig. 3. Note that as the rf motion is coherent, this distortion does not affect the ion temperature. However, the resulting elongation can cause part of the ion distribution to fall outside the confines of the ion guide. In order to minimize this effect, the operating parameters of the ion guide have to be

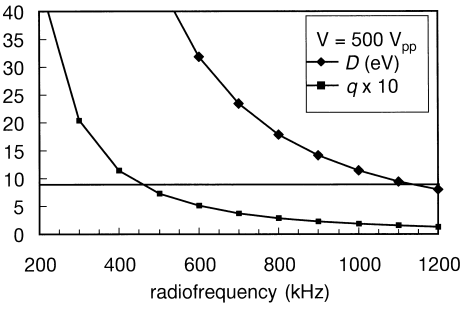

Fig. 4. Variation of the Mathieu stability parameter q and the potential well depth D (eV) for $^{133}Cs^+$ as a function of applied rf frequency for an applied rf voltage of 500 V_{pp} (note the axis is multiplied by 10 for q). The horizontal line shows the corresponding stability limit of $q = 0.9$. The game is to maximize D (for good confinement) and minimize q (to avoid rf distortion).

chosen carefully. First, reducing the effect of the rf can be done simply by lowering the rf voltage. However this has the disadvantage of also lowering the ion guide confining power, or potential well depth D, given by $D = \frac{1}{4}qV$. Therefore, we must minimize q and maximize D which results in choosing a rf voltage as high as possible (limited by a discharge in the buffer gas) and a rf frequency such that q remains modest (less than about 0.5). This effect is illustrated in Fig. 4. For this simulation we have used a $^{133}Cs^+$ ion, a rf voltage of 500 V_{pp}, and a frequency of 0.6 MHz which results in $q = 0.5$ and $D = 32$ eV. The resulting macromotion frequency ω_0 is 108 kHz as calculated from: $\omega_0 \approx (1/2\sqrt{2})q\Omega$.

The effect of rf distortion is illustrated in Fig. 5 by the calculated phase space diagrams for various phases of rf at injection. The elongation of the original ellipse at the entrance of the guide (also shown) is easily seen and it shows that indeed, some of the ions would be lost before having their motion adequately damped by the buffer gas. However, if we recall the ion distribution shown in Fig. 3, the number of ions present in the wings is relatively small so that the resulting loss in transmission would be only about 15%. This loss could be remedied by a simple bunching voltage added to the injection electrode in order to let the ions arrive at a rf phase where rf distortion is minimized as illustrated in Fig. 5 by the later rf phases. Such a bunching scheme has been proposed for injection into Paul traps by Moore and Gulick [10].

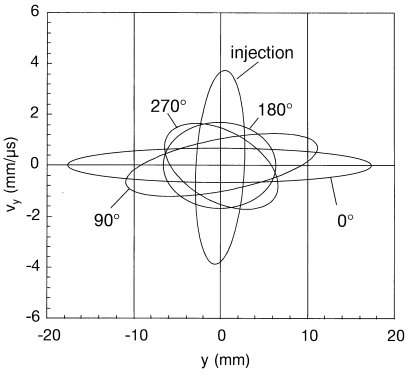

Fig. 5. Evolution of the transverse (y coordinate) phase space diagram of the decelerated $^{133}Cs^+$ beam when subjected to the quadrupole field of the rf ion guide (without buffer gas) at various phases of the rf. The applied rf frequency is 0.6 MHz and rf voltage 500 V_{pp} for the beam shown in Fig. 2 (initial energy 130 eV, beam diameter 7 mm, and divergence 15°). Dotted lines show the limits of the ion guide electrodes. Early phases (0–90°) show that some ions (15%) are lost but later phases (180–270°) show that with prebunching, 100% transmission would be possible.

3.4. Buffer gas cooling by viscous damping

The viscous damping term is calculated using a parameter function fit of measurement data from ion mobilities in gases [11] which are tabulated versus ion drift velocity. Mobility (or gas transparency) is the proportionality constant between an applied electric field and the resulting drift velocity (as the ion is no longer accelerated at the pressures in question). The mobility concept ceases to be useful when ion energies become very large compared to thermal energies, and at this point the damping coefficient is modeled using the mean-free path and reduced mass of the ion and gas atom. The mobility parameter function takes the form: $K_0 = 1/(c_1 + c_2 v + c_3 v^2)$ where c_1, c_2 and c_3 are fitting constants, v is the ion velocity, and K_0 is the reduced ion mobility (expressed in m^2/V s). The ion mobility K is normalized to a given temperature T and pressure p relative to standard temperature T_N and pressure p_N by: $K = K_0(T/T_N)/(p/p_N)$. An example of this function is shown in Fig. 6 for K^+ ions in He gas at 1×10^{-4} Torr. For comparison, the "equivalent mobility" K_{hb} for a hard ball collision is also shown and is calculated using:

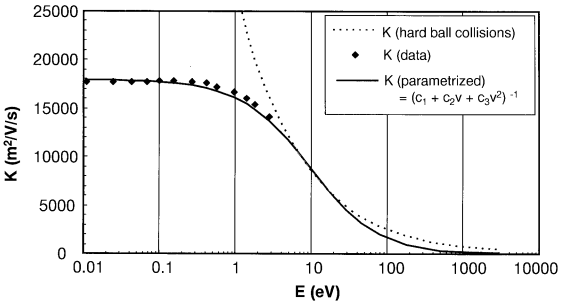

Fig. 6. The mobility of $^{39}K^+$ in He versus kinetic energy for a pressure of 1×10^{-4} Torr (mobility data points are from [11]). Also shown is the mobility calculated using the gas-kinetic cross section ($\sigma \approx 3 \times 10^{-19}$ m^{-2}). Note: the damping parameter function uses velocity though energy and is shown here for convenience (fitting parameters used: $c_1 = 0.0455$, $c_2 = 5 \times 10^{-7}$, $c_3 = 9 \times 10^{-10}$).

$$K_{hb} = \frac{2e}{m_{ion}} \frac{(m_{ion} + m_{gas})^2}{m_{ion} m_{gas}} \frac{1}{n\sigma v} \quad (2)$$

where n is the gas density and σ is the elastic collision cross section for hard-ball collisions. At higher energies, one can see that the measured mobility approaches the hard ball one and indeed, the fit is tailored to follow this curve at higher energies. There is a preponderance to treat buffer gas collisions as hard-ball collisions which is not correct for ions of thermal energies as can be seen from the graph. Evidence for this claim can be found from cooling times observed for ions in Paul traps [9] which are much shorter that what would seem possible from hard-ball collisions as shown in Fig. 7. Still further support for viscous damping calculated from measured mobilities can be found from measurements of buffer gas cooling in Penning traps [12]. In fact, viscous damping is produced by the long-range induced-dipole interaction by which an ion feels the effect of many gas atoms at once rather than the very short range force of a direct collision [11].

The acceleration term in the numerical integration thus subtracts the mobility calculation illustrated above which is recalculated using the new velocity after each step. As the final energy of the cooled ions should be in equilibrium with the gas, the corresponding room temperature energy is also added to the acceleration term after each step (otherwise the

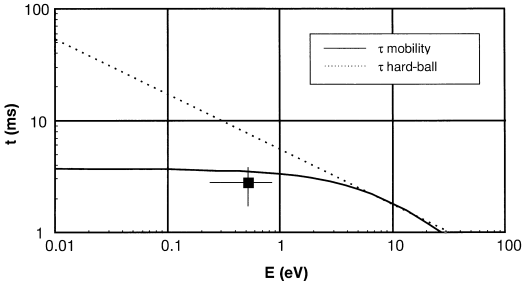

Fig. 7. Cooling time t of $^{39}K^+$ in He versus kinetic energy E for a pressure of 1×10^{-4} Torr calculated from the ion mobility fit of Fig. 7 (solid line) and from the gas-kinetic cross section (dotted line). The data point corresponds to a range of cooling time measurements made in a Paul trap [9] for these conditions.

motion would be cooled to zero). This is done using the macromotion frequency ω_0 which represents the statistical motion of the ions [9]. This frequency is calculated from the operating parameters. The final acceleration term is therefore:

$$\ddot{y} = \frac{e}{m}\left(\frac{V\cos(\Omega t - \phi)}{x_0^2}y - \frac{\dot{y}}{K} + \frac{v_{th}}{K_{th}}\cos(\omega_0 t)\right) \quad (3)$$

where v_{th} is the velocity of mass m corresponding to the chosen temperature (300 K) and K_{th} is the mobility corresponding to v_{th}. Note that for z, the first term is zero and the last term is constant, leaving only a "diffusion" velocity. This formulation implicitly assumes that the ion direction is not changed after a collision. The consequences of including both velocity and time inside the acceleration make the integration unstable at high pressures but if care is taken with the step size, the error behaves normally.

3.5. Buffer gas pressure and pumping considerations

In principle, the higher the buffer gas pressure, the faster the cooling will take place and the shorter the guide can be. The pressure is, of course, limited not only by the voltages needed on the rods (and deceleration electrodes), but by the pumping capacity. Calculations were done to have some idea of what buffer gas pressures would be feasible. As shown in the schematic diagram of Fig. 1, we foresee a turbomolecular pump at each end of the quadrupole ion guide system. A typical pumping speed S of 500 L/s is assumed. Using Knudsen's formula, the vacuum impedance L (in L/s) of a cylinder of diameter d and length l can be calculated using:

$$L = 135\frac{d^4}{l}\bar{p} + 12.1\frac{d^3}{l}\frac{1 + 192d\bar{p}}{1 + 237d\bar{p}} \quad (4)$$

where $\bar{p} = \frac{1}{2}(p_1 + p_2)$ for an entrance pressure p_1 and exit pressure p_2. The two terms in the equation correspond to laminar and molecular flow. If we simply equate the product of the pumping speed and the exit pressure p_2 to the flow, $L(p_1 - p_2)$, various combinations of geometry and pressure gradients can be evaluated. Results of some such evaluations are listed in Table 1. Note that here we assume the quadrupole is a closed structure so that the pressure is determined by the conductance. In the case of an open structure, the pressure is determined by the apertures at the ends. In the gas flow range investigated here,

Table 1
Pumping speeds S calculated from Knudsen's formula in Eq. (4) considering a simple tube of length l and diameter d for pressure p_1 at entrance and p_2 at exit. The gas is introduced into the center of the quadrupole but the calculation here uses the geometrical symmetry meaning that p_2 will correspond to the pressure in the center. The values in row 4 were used in the simulation (at these pressures the flow is approximately 20% laminar and 80% molecular)

p_1 (mbar)	p_2 (mbar)	l (cm)	d (cm)	L (L/s)	S (L/s)
1.0E + 01	1.0E − 06	100	0.1	0.001	7730
5.0E − 01	5.0E − 06	100	0.5	0.033	3340
3.3E − 02	1.0E − 05	25	1.0	0.500	1650
3.3E − 02	3.3E − 05	25	1.0	0.500	500
1.0E − 02	1.0E − 05	25	1.0	0.461	460
1.0E − 03	2.0E − 06	25	1.0	0.477	240
1.0E − 03	3.0E − 06	25	1.0	0.477	160

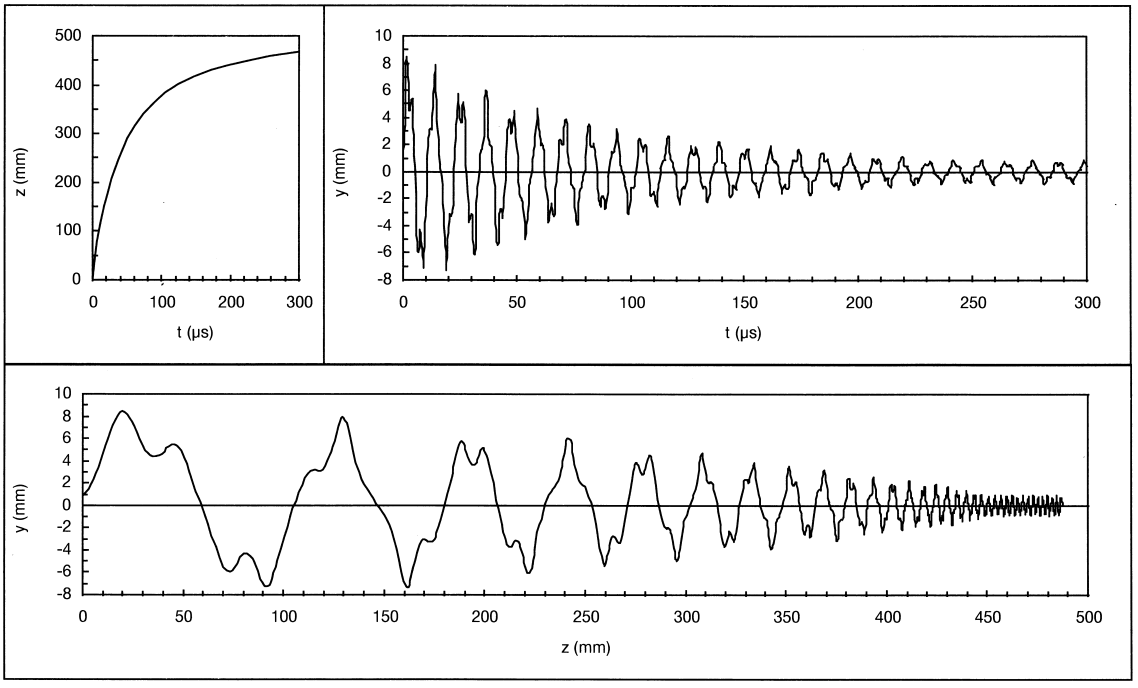

Fig. 8. Simulated trajectory of a single $^{133}Cs^{+}$ ion with an axial energy of 130 eV and a transverse energy of 8.5 eV in the presence of 0.033 Torr of He buffer gas in a quadrupole ion guide. The trajectories of both y and z versus t are plotted as well as y versus z. The motion is quickly damped in both dimensions corresponding to an ion guide length of less than 50 cm. Ion guide operating parameters are: $x_0 = 10$ mm, $V = 250\ V_{op}$, $f = 0.6$ MHz. Note the residual transverse oscillation due to the thermal velocity and the "diffusion velocity" in the longitudinal coordinate. The total transit time is less than 0.4 ms.

the pressures for open and closed structures turn out to be approximately the same.

4. Results and discussion

Using the ion guide parameters given above and the action diagram calculated by SIMION, it was found that a 50 cm long ion guide operated at a pressure of 0.033 Torr of He could cool the Cs ions to room temperature in all three dimensions. The calculated ion trajectory for a corner point on the action diagram is shown in Fig. 8. The ion is damped in the transverse coordinate with a time constant of about 100 μs. In the longitudinal direction this is achieved in less than 50 μs (due to the higher initial velocity). A test was also made using an initial longitudinal energy spread of 10 eV and all the ions were cooled to the temperature of the gas, thus eliminating the spread.

While Fig. 8 is interesting for the form of the trajectory inside the ion guide, it gives us only an indication that the emittance has been reduced as a result of the cooling but nothing quantitative. To get a number, we must compare the action diagrams at the entrance and exit of the ion guide, as done in Fig. 9. Here the input and output phase space diagrams—directly proportional to the emittances—are superimposed. When the emittance is calculated from these diagrams ($\pi/4 \times \delta y \times \delta\theta$) and then normalized for the beam transport energy, we get a reduction factor of about 100 (for each coordinate).

In principle the emittance reduction is simply determined by the ratio of the temperature corresponding to the energy spread in the ion source to that of the buffer gas. For an ISOLDE beam this corresponds to a few eV compared to 0.026 eV if a room-temperature gas is used. This corresponds roughly to what we see

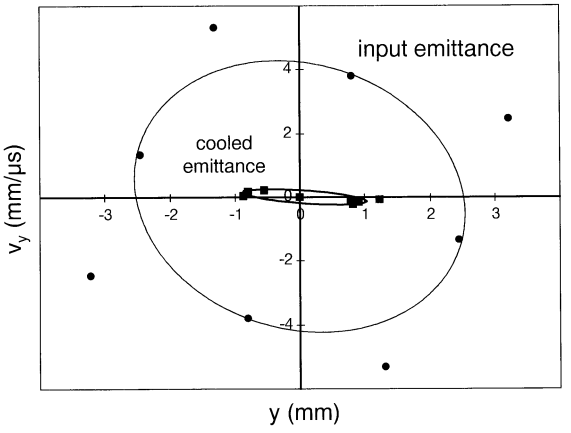

Fig. 9. Transverse phase space (action area) diagrams (for one dimension) of the ion beam before and after transit through the collisional cooling system. The ratio of the corresponding emittances is a factor of 100. Note that there are the same number of particles in each ellipse! The initial phase space area was that generated by SIMION using the electrode configuration of Fig. 2.

here and which is what we should expect. However, it is important that the conditions under which this is done be well controlled and that the final emittance, although smaller, must be usefully distributed and that the number of particles remains the same.

All of the operating parameters are very tightly coupled and therefore, several iterations are required before finding values that are compatible for overall optimization. Given an initial emittance, one has to decide what spot size to focus on, thus imposing the divergence which requires a particular ion guide potential well depth. The entrance aperture (which also affects the potential well) determines the vacuum conductance and thus a required length in order to respect the pumping speed given a pressure that will damp the ions within this length, and this pressure must in turn be not so high as to cause a discharge inside the quadrupole.

Although the parameters have not yet been exhaustively studied, these preliminary results show that such a system is definitely feasible. For the moment, the critical problem seems to be the transmission loss due to rf distortion and perhaps the gas load on the system. The loss of ions due to charge exchange and other chemical reactions also has not been evaluated. This is sure to play some role as previous results have already shown [5,13]. Another factor not considered here is the phenomenon of rf heating that occurs in Paul traps. This effect causes an increase in temperature (and hence, emittance) when collisions with heavier ions cause a transfer of the coherent rf motion to the statistical (macro) motion. rf heating depends predominantly on the base pressure and cleanliness of the vacuum system. Thus, there is an urgent need to perform preliminary experimental studies in order to verify many of the assumptions used in the simulation. A test system scaled-down by a factor of 10 in energy has now been built to pursue this.

A complementary experimental program has been established at McGill University using a surface ionization source and a mass filter (with an axial field) operated at up to 1 Torr of He. Transmissions better than 80% have been achieved through a 1 mm hole with the beam energy spread not exceeding 0.2 eV for a 1 kV beam [14].

References

[1] Mass measurements at Isolde using a transmission radiofrequency spectrometer on-Line (IS-346). See M.D. Lunney et al. Hyp. Int. 99 (1996) 105. ISOLDE is the Isotope Separator On Line at CERN, the European Organization for Nuclear Research.
[2] (a) M.D. Lunney, F. Buchinger, R.B. Moore, J. Mod. Opt. 39 (1992) 349; (b) W.M. Itano, J.C. Bergquist, J.J. Bollinger, D.J. Wineland, Phys. Scr. T59 (1995) 106.
[3] D.J. Douglas, J.B. French, J. Am. Soc. Mass Spectrom. 3 (1992) 398.
[4] H.J. Xu, M. Wada, J. Tanaka, H. Kawakami, I. Katayama, S. Ohtani, Nucl. Instrum. Methods Phys. Res. A 333 (1993) 274.
[5] P. Van den Bergh et al. Nucl. Instrum. Methods Phys. Res. A 333 (1996) 194.
[6] M. de Saint Simon, CERN Internal Report ISC/P54 Add. 2, 1994.
[7] Quadrupole Mass Spectrometry and its Applications, P.H. Dawson (Ed.), Elsevier Scientific, Amsterdam, 1976.
[8] R.B. Moore, A.-M. Ghalambor Dezfuli, P. Varfalvy, H. Zhao, Phys. Scr. T59 (1995) 93.
[9] M.D. Lunney, Ph.D. thesis, McGill University, Montreal, 1992, unpublished.
[10] R.B. Moore, S. Gulick, Phys. Scr. T22 (1988) 28.
[11] L.A. Viehland, E.A. Mason, At. Data Nucl. Data Table 60 (1995) 37, and references therein.
[12] M. Koenig, G. Bollen, H.-J. Kluge, T. Otto, J. Szerypo, Int. J. Mass Spectrom. Ion Processes 142 (1995) 95.
[13] H. Backe et al. in T. Von Egidy, D. Habs, F.J. Haartmann, K.E.G. Loebner, H. Nifenecker (Eds.), Proceedings of the International Workshop on Research with Fission Fragments, Benediktbeuern, 28–30 October 1996, p. 80.
[14] T. Kim, Ph.D. thesis, McGill University, Montreal, 1997, unpublished.